

Transport in very dilute solutions of ^3He in superfluid ^4He

Gordon Baym,^{a,b} D. H. Beck,^a and C. J. Pethick^{a,b,c}

^a*Department of Physics, University of Illinois, 1110 W. Green Street, Urbana, IL 61801*

^b*The Niels Bohr International Academy, The Niels Bohr Institute,
Blegdamsvej 17, DK-2100 Copenhagen Ø, Denmark*

^c*NORDITA, KTH Royal Institute of Technology and Stockholm University, Roslagstullsbacken 23, SE-10691 Stockholm, Sweden*

(Dated: April 12, 2018)

Motivated by a proposed experimental search for the electric dipole moment of the neutron (nEDM) utilizing neutron- ^3He capture in a dilute solution of ^3He in superfluid ^4He , we derive the transport properties of dilute solutions in the regime where the ^3He are classically distributed and rapid ^3He - ^3He scatterings keep the ^3He in equilibrium. Our microscopic framework takes into account phonon-phonon, phonon- ^3He , and ^3He - ^3He scatterings. We then apply these calculations to measurements by Rosenbaum et al. [J. Low Temp. Phys. **16**, 131 (1974)] and by Lamoreaux et al. [Europhys. Lett. **58**, 718 (2002)] of dilute solutions in the presence of a heat flow. We find satisfactory agreement of theory with the data, serving to confirm our understanding of the microscopics of the helium in the future nEDM experiment.

PACS numbers: 67.60.G- 13.40.Em

I. INTRODUCTION

Dilute solutions of ^3He in superfluid ^4He have been an ideal testing ground for theories of quantum liquids, with past focus generally on ^3He concentrations and temperatures for which the ^3He forms a degenerate Fermi gas. The proposed use of ultra-dilute solutions in the search for a neutron electric dipole moment (nEDM) at the Oak Ridge National Laboratory Spallation Neutron Source (SNS) [1, 2], as well as earlier experiments by Rosenbaum et al. [3] and by Lamoreaux et al. [4], all require careful treatment of the transport properties of the solutions. The characteristic temperatures in all cases considered here are of order 0.5 K, at which phonons are the dominant excitation of the ^4He . In the low temperature degenerate ^3He regime, phonons have small effect on the ^3He properties. However, with increasing dilution, when the ^3He become classically distributed, the situation is reversed, and the phonons play a more and more important role. In the proposed nEDM experiment, a crucial issue is to be able to periodically sweep out the ^3He by imposing a temperature gradient [5]; the underlying physics of the transport is scattering of phonons in the superfluid ^4He against the ^3He . The Lamoreaux et al. experiment, which measured the effect of a heat source on the steady state distribution of ^3He atoms in a dilute solution, was a prototype for the effects of a “phonon wind” on the ^3He . The Rosenbaum et al. experiment measured the thermal conductivity of dilute solutions as a function of temperature and concentration. We show below that the results of these experiments can be understood in terms of a simple thermal conductivity determined using well-established scattering amplitudes.

In the experiments of Refs. [3] and [4], the ^3He number concentrations, $x_3 = n_3/(n_3 + n_4)$, where n_3 and n_4 are the ^3He and ^4He number densities, are in the range 7×10^{-5} to 1.5×10^{-3} in the non-degenerate regime. Here

momentum carried by the phonons goes primarily into the ^3He , which then transfer it to the walls. The physical dimensions of the experimental container are sufficiently large that the transport properties are determined locally by the microscopic scatterings of the ^3He and the phonons. The ^3He - ^3He interactions are sufficiently strong that they keep the ^3He in thermal equilibrium at rest at the local temperature $T(\vec{r})$, while phonon-phonon interactions keep the phonons in drifting local equilibrium. By contrast, in the proposed SNS experiment, phonon momentum is transferred primarily to the walls by viscous forces, with the ^3He playing a negligible role. Furthermore, collisions of ^3He with the phonons are responsible for establishing equilibrium in the ^3He cloud. A common characteristic of these experiments is the effect on the dilute solution produced by a localized, static heat source. In this paper we focus on calculating transport properties in the higher concentration regime in Refs. [3] and [4], where the fact that the ^3He - ^3He mean free path is short greatly simplifies the transport theory. At lower ^3He concentrations, $x \lesssim 10^{-6}$, the transport must be calculated by solving the coupled Boltzmann equations for the phonons and ^3He , taking into account viscous forces at the boundaries; these results as well as their impact on the transport of ^3He in the much lower concentration regime of the SNS nEDM experiment will be described elsewhere [6].

In Sec. II we examine the hydrodynamic constraints deriving from the steady state situation and from the properties of the superfluid. The basic scattering mechanisms determining the transport properties of dilute solutions— ^3He - ^3He , ^3He -phonon, and phonon-phonon interactions—are described in Sec. III. In Sec. IV, we calculate the thermal conductivity (dominated by the phonons) in this situation; in this calculation we include inelastic recoil of the ^3He in scattering against the phonons (detailed in Appendix A). We find that, contrary to the earlier treatment in Ref. [7] used by Rosenbaum

et al., the rapid relaxation of phonons along rays of constant phonon direction dominates their distribution [8]. We calculate the conductivity by considering the drag force on the phonons due to their scattering against the stationary ^3He , using the method close in spirit to that introduced earlier in a calculation of the mobility of ions in superfluid ^4He [9], and later used by Bowley [10] in his accounting of the Lamoreaux et al. experiment. Despite a superficial similarity of the present approach to these earlier calculations, the underlying physics is different here. In Sec. V, we show how the microscopic theory satisfactorily explains the experimental findings in both the Rosenbaum et al. and the Lamoreaux et al. experiments.

II. RESPONSE TO STATIC DISTURBANCES

To understand how dilute solutions respond to a localized static heat source, the physical mechanism of interest in the experiments, we first review the hydrodynamics of the solutions. At low temperatures the phonons are the dominant excitations of the ^4He , and the momentum density or mass current density of the ^4He is

$$\vec{g}_4 = \rho_s \vec{v}_s + \rho_{ph} \vec{v}_{ph}, \quad (1)$$

where \vec{v}_s is the superfluid flow velocity, \vec{v}_{ph} is the phonon fluid flow velocity, ρ_s is the superfluid mass density, and

$$\rho_{ph} = \frac{2\pi^2 T^4}{45 s^5} \quad (\ll \rho_s) \quad (2)$$

is the ^4He normal fluid density. Similarly, the ^3He momentum density is

$$\vec{g}_3 = \rho_3 \vec{v}_3, \quad (3)$$

where \vec{v}_3 is the ^3He flow velocity, and $\rho_3 = m^* n_3$, with $m^* = m_3 + \delta m \simeq 2.34 m_3$ the effective mass [7]. The total mass current, \vec{g} , is $\vec{g}_4 + \vec{g}_3$.

When the ^4He mass flow vanishes, $|v_s| = (\rho_{ph}/\rho_s) |v_{ph}| \ll |v_{ph}|$ at temperatures $\lesssim 0.6$ K, and the only relevant flow velocities are those of the phonons and possibly the ^3He . Then force balance in the dilute solutions implies that to linear order,

$$\nabla P = \eta_{ph} \nabla^2 \vec{v}_{ph} + \eta_3 \nabla^2 \vec{v}_3, \quad (4)$$

where $P = P_3 + P_{ph}$ is the total pressure, with $P_3 = n_3 T$ the ^3He partial pressure (we generally work in units with \hbar and Boltzmann's constant, k_B , equal to unity), T is the temperature, P_{ph} is the phonon partial pressure, η_{ph} is the first viscosity of the normal fluid and η_3 the first viscosity of the ^3He . (In the situations of interest, in a steady state, $\nabla \cdot \vec{v}_{ph}$ and $\nabla \cdot \vec{v}_3$ both vanish.) For a container large compared with microscopic viscous mean free paths, and for ^3He concentrations in the range of those in Refs. [3] and [4], both viscosity terms are insignificant compared with the drag forces between the ^3He and the

phonons, as we discuss in Sec. IV, and thus can be neglected. (At the much lower ^3He concentrations of the proposed SNS experiment, however, the phonon viscosity does play a significant role [6].) The total pressure is effectively constant throughout the system, $\nabla P = 0$.

In addition, as one sees from the linearized superfluid acceleration equation [11],

$$m_4 \frac{\partial \vec{v}_s}{\partial t} + \nabla \mu_4 = 0, \quad (5)$$

the ^4He chemical potential, μ_4 , is constant in a steady state. The Gibbs-Duhem relation for the solutions, $\nabla P = n_4 \nabla \mu_4 + n_3 \nabla \mu_3 + S \nabla T$, with μ_3 the ^3He chemical potential, T the temperature, and S the total entropy density, together with the constancy of the pressure and the relation, $\nabla P_3 = n_3 \nabla \mu_3 + S_3 \nabla T$ (which neglects the effects of ^3He -phonon interactions on the thermodynamics, e.g., small terms in the total pressure of order $P_{ph} n_3 / n_4 \ll P_{ph}$), then implies that

$$\nabla P_3 + S_{ph} \nabla T = 0, \quad (6)$$

where $S_{ph} = 4P_{ph}/T$ is the phonon entropy density, and $dP_{ph} = S_{ph} dT$. Equation (6) and the foregoing then give the simple relation between the temperature and ^3He density gradients in the system:

$$\nabla T = -\frac{T}{S_{ph} + n_3} \nabla n_3; \quad (7)$$

in a steady state a gradient of the ^3He density is always accompanied by a gradient of the temperature. (Note that the n_3 in the denominator arises when one consistently includes a non-zero temperature gradient at every step of the calculation, unlike in earlier studies [13, 14] where the ^3He pressure was tacitly assumed to obey $dP_3 = T dn_3$.) A heat flux, \vec{Q} , in the system is related to the temperature gradient by $\vec{Q} = -K \nabla T$, where K is the thermal conductivity of the solution. Thus Eq. (7) relates the ^3He density gradient to the heat flux by

$$\nabla n_3 = \frac{S_{ph} + n_3}{TK} \vec{Q}. \quad (8)$$

The ^3He density on the right can be significant. Since

$$TS_{ph} = s^2 \rho_{ph} \quad (9)$$

one has

$$\frac{n_3}{S_{ph}} = 300 \frac{x_3}{T^3}, \quad (10)$$

with T measured in K; at $T = 0.45$ K and $x_3 = 3 \times 10^{-4}$ the ratio is unity.

We note that, in general, the response to a heat current in a steady state is a temperature gradient with the constant of proportionality being the thermal conductivity; the particle current in general depends on both gradients of concentration and temperature [15]. In

the present case, because of the relation between ∇n_3 and ∇T , Eq. (7), the ^3He diffusion coefficient is proportional to the thermal conductivity and thus the results of Ref. [4] can also be described in terms of a diffusion coefficient. However, when viscous effects become important (for $x_3 < 10^{-6}$), Eq. (7) is no longer valid and the thermal conductivity and diffusion constant are not related in a simple way [6]. In the following we will generally talk about the response to a heat current in terms of the thermal conductivity.

III. MICROSCOPIC SCATTERING PROCESSES

The microscopic processes that determine the transport properties of dilute solutions are ^3He - ^3He [16], phonon-phonon [8], and phonon- ^3He [7] scatterings; the amplitudes of these processes have been well studied in earlier helium research. At low energies, the total cross section for a ^3He atom scattering from a second ^3He atom of opposite spin can be written as

$$\sigma_{33} = \frac{9\pi^3}{k_D^2} v_{33,0}^2 \left(\frac{m^*}{m_4}\right)^2 \left(\frac{m_4 s}{k_D}\right)^4 = 10.3 \text{ \AA}^2, \quad (11)$$

where k_D is the Debye wave number, defined by $n_4 = k_D^3/6\pi^2$, and $v_{33,0} = -0.064$ measures the strength of the ^3He - ^3He interaction at zero momentum transfer [16]. Phonon-phonon scattering rates at forward angles [8] are rapid compared with phonon- ^3He rates. While such scatterings do not directly affect the heat current, they do play the important role of keeping the phonon momentum distribution, $n_{\vec{q}}$, in local thermodynamic equilibrium with a drift velocity, \vec{v}_{ph} ,

$$n_{\vec{q}} = \frac{1}{e^{(sq - \vec{q} \cdot \vec{v}_{ph})/T} - 1}. \quad (12)$$

This is the key difference between the current treatment and that in Refs. [3] and [7], where it is assumed that the phonon- ^3He scattering dominates the phonon relaxation.

The amplitude for scattering of a phonon of wavevector \vec{q} against a ^3He of wavevector \vec{p} to final states \vec{q}' and \vec{p}' is determined theoretically in terms of the measured excess volume, α , of a ^3He atom compared with that of a ^4He atom and the ^3He effective mass, m^* . The scattering amplitude is approximately [7]

$$\langle p'q' | T | pq \rangle = \frac{s(qq')^{1/2}}{2n_4} (A + B \cos \theta), \quad (13)$$

where θ is the angle between \vec{q}' and \vec{q} , $A = n_4 d\alpha/dn_4$ and $B = (1 + \alpha + \delta m/m_4)(m_4/m^*)(1 + \alpha - m_3/m_4)$.

At very low temperatures, $T \ll 1$ K, the scattering can taken to be elastic. The momentum dependent scattering rate of phonons from the ^3He is then [6]

$$\gamma_3(q) = \frac{sq^4 x_3}{4\pi n_4} J, \quad (14)$$

where

$$J = A^2 + B^2/3 - 2AB/3; \quad (15)$$

the q^4 in this rate is characteristic of Rayleigh scattering. More generally, as Bowley emphasized [10], recoil of the ^3He in scattering produces a significant correction to the effective phonon- ^3He scattering rate [17]. As we show in Appendix A, ^3He recoil corrections to the result (14) are of relative order $T/1.36$ K.

We now estimate the importance of 3-3 versus phonon scattering in bringing the ^3He into equilibrium. The mean free path of a ^3He scattering on unpolarized ^3He is

$$\ell_{33} = \frac{2}{n_3 \sigma_{33}} = \frac{8.66 \times 10^{-8}}{x_3} \text{ cm}; \quad (16)$$

the factor $n_3/2$ is the density of opposite spin ^3He . Similarly, the mean free path for scattering of ^3He of momentum p on phonons is given approximately by $p^3/m\Gamma$, where

$$\begin{aligned} \Gamma &= \frac{1}{n_3} \int \frac{d^3q}{(2\pi)^3} q^2 \gamma_3(q) n_q^0 (1 + n_q^0) \\ &= 270\pi J \left(\frac{S_{ph}}{n_4}\right)^2 \frac{T^3}{s^2} \sim T^9, \end{aligned} \quad (17)$$

in the limit $p \gg q$. Here $n_q^0 = (e^{sq/T} - 1)^{-1}$ is the equilibrium phonon distribution function. Replacing p^2 by $3m^*T$, an appropriate thermal average, we find

$$\begin{aligned} \ell_{3ph} &= \frac{\sqrt{3}}{2J} \left(\frac{S_{ph}}{n_4}\right)^2 \frac{m^{*1/2} s^2}{T^{3/2}} \\ &= 0.077 \left(\frac{0.45 \text{ K}}{T}\right)^{15/2} \text{ cm}. \end{aligned} \quad (18)$$

Comparing the mean free paths (16) and (18), we find

$$\frac{\ell_{3ph}}{\ell_{33}} = 0.89 \times 10^6 x_3 \left(\frac{0.45 \text{ K}}{T}\right)^{15/2}. \quad (19)$$

For $T = 0.45$ K and $x_3 = 10^{-6}$, $\ell_{3ph} \approx \ell_{33}$, while for $T = 0.65$ K and $x_3 = 3 \times 10^{-4}$, $\ell_{3ph}/\ell_{33} \approx 16.9$. Thus for $T \sim 0.5$ K, and $x_3 \sim 10^{-5}$ a good first approximation is to assume that scattering of ^3He by ^3He atoms is fast compared with scattering of ^3He by phonons. In fact, as will be shown in detail in [6], we may take the momentum distribution of the ^3He to be simply that of a classical gas in equilibrium and at rest,

$$f_p^0 = e^{-(p^2/2m^* - \mu_3)/T}. \quad (20)$$

IV. THERMAL CONDUCTIVITY

The thermal conductivity of the dilute solutions can in general be calculated by solving the coupled phonon and

^3He Boltzmann equations to determine the steady state momentum distributions of the phonons and the ^3He , and, from these distributions, the heat and particle currents. However, here, where the ^3He are approximately stationary and in equilibrium, the phonon thermal conductivity can be found simply, by calculating the rate at which the phonons lose momentum by scattering against ^3He [9, 10].

In a steady state the net force density on the phonons drifting at velocity \vec{v}_{ph} is balanced by the phonon pressure gradient, $\nabla P_{ph} = S_{ph}\nabla T$. Microscopically then,

$$\begin{aligned} \nabla P_{ph} = & - \int \frac{d^3q}{(2\pi)^3} \int \frac{d^3q'}{(2\pi)^3} \int 2 \frac{d^3p}{(2\pi)^3} \\ & \times \vec{q} |\langle \mathcal{T} \rangle|^2 2\pi\delta(sq + p^2/2m^* - sq' - p'^2/2m^*) \\ & \times [f_p^0 n_{\vec{q}}(1 + n_{\vec{q}'}) - f_{p'}^0 n_{\vec{q}'}(1 + n_{\vec{q}})], \end{aligned} \quad (21)$$

where $\vec{p}' - \vec{p} = \vec{q} - \vec{q}' \equiv \vec{k}$, $\langle \mathcal{T} \rangle = \langle p'q' | \mathcal{T} | pq \rangle$, $n_{\vec{q}}$ is the phonon distribution, and the factor of 2 is from the ^3He spin sum. In terms of the ^3He structure function,

$$\begin{aligned} S_3(k, \omega) = & 2 \int \frac{d^3p}{(2\pi)^3} \delta(\omega + p^2/2m^* - p'^2/2m^*) f_p^0, \\ = & n_3 \left(\frac{m^*}{2\pi k^2 T} \right)^{1/2} e^{-m^*(\omega - k^2/2m^*)^2/2k^2 T}, \end{aligned} \quad (22)$$

which obeys $S_3(k, -\omega) = e^{-\omega/T} S_3(k, \omega)$, we can rewrite Eq. (21) as,

$$\begin{aligned} \nabla P_{ph} = & - \int \frac{d^3q}{(2\pi)^3} \int \frac{d^3q'}{(2\pi)^3} \int_{-\infty}^{\infty} d\omega \\ & \times \vec{q} |\langle \mathcal{T} \rangle|^2 2\pi\delta(\omega - sq + sq') S_3(k, \omega) \\ & \times [n_{\vec{q}}(1 + n_{\vec{q}'}) - n_{\vec{q}'}(1 + n_{\vec{q}}) e^{-\omega/T}]. \end{aligned} \quad (23)$$

Since $n_{\vec{q}'}(1 + n_{\vec{q}}) = n_{\vec{q}}(1 + n_{\vec{q}'})e^{(\omega - \vec{k} \cdot \vec{v}_{ph})/T}$, the final line in Eq. (23) to first order in v_{ph} is $n_{\vec{q}}^0(1 + n_{\vec{q}'}^0)(\vec{k} \cdot \vec{v}_{ph})/T$. Finally, symmetrizing the integrand in q and q' , and carrying out the angular averages, we have, in agreement with Bowley,

$$\begin{aligned} \nabla P_{ph} = & - \frac{\vec{v}_{ph}}{6T} \int \frac{d^3q}{(2\pi)^3} \int \frac{d^3q'}{(2\pi)^3} n_q^0(1 + n_{q'}^0) k^2 |\langle \mathcal{T} \rangle|^2 \\ & \times \int_{-\infty}^{\infty} d\omega 2\pi\delta(\omega - sq + sq') S_3(k, \omega). \end{aligned} \quad (24)$$

Neglecting ^3He recoil is equivalent to setting $S_3(k, \omega) = n_3\delta(\omega)$. In this case,

$$\begin{aligned} \nabla P_{ph} = & - \frac{\vec{v}_{ph}}{6T} \int \frac{d^3q}{(2\pi)^3} \int \frac{d^3q'}{(2\pi)^3} n_q^0(1 + n_{q'}^0) k^2 |\langle \mathcal{T} \rangle|^2 \\ & \times 2\pi\delta(sq - sq'), \\ = & - \frac{n_3\Gamma}{3T} \vec{v}_{ph} = - \frac{8\pi^5 x_3 J}{45 n_4} \left(\frac{T}{s} \right)^8 \vec{v}_{ph}. \end{aligned} \quad (25)$$

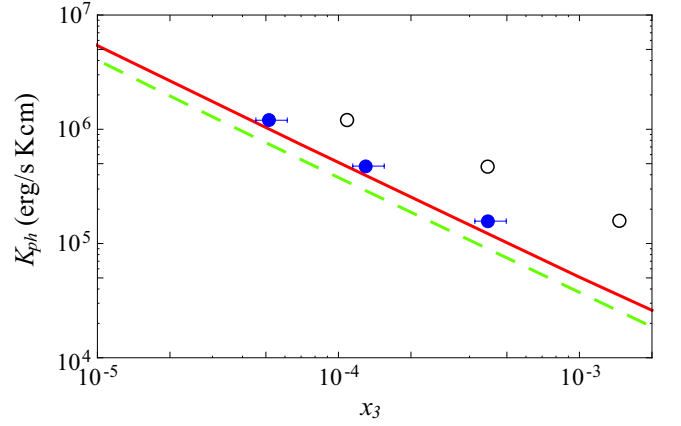


FIG. 1: (Color online) Thermal conductivity of a dilute solution of ^3He in superfluid ^4He at $T = 0.45$ K. The solid line shows the phonon thermal conductivity, in the limit in which the ^3He are at rest in equilibrium, calculated with ^3He recoil (see text). The dashed line shows the phonon thermal conductivity, Eq. (27), without recoil corrections. The open circles are three representative measurements at $T \sim 0.43$ K at the average x_3 reported in Ref [3]; the solid circles with the error bars are the same thermal conductivities, but shown at the corrected x_3 , as discussed in Sec. VI.

The phonon heat current density,

$$\vec{Q}_{ph} = s^2 \int \frac{d^3q}{(2\pi)^3} \vec{q} n_{\vec{q}} = T S_{ph} \vec{v}_{ph}, \quad (26)$$

in steady state determines the phonon thermal conductivity, $\vec{Q}_{ph} = -K_{ph}\nabla T$, and since $\nabla P_{ph} = S_{ph}\nabla T$, we find the simple result [18]

$$K_{ph} = S_{ph} s \ell_{ph3} = \frac{3T^2 S_{ph}^2}{n_3\Gamma} = \frac{n_4 s^2}{90\pi x_3 J T}, \quad (27)$$

where $\ell_{ph3} = 3T^2 S_{ph}/n_3\Gamma$ defines an effective mean free path for phonons scattering on ^3He .

In Appendix A we include ^3He recoil to leading order in T/m^*s^2 , which we find increases the thermal conductivity by $\sim 25-35\%$ in the range $T = 0.45-0.65$ K. Figure 1 shows the phonon thermal conductivity computed from Eq. (A15), as well as the approximate thermal conductivity, Eq. (27) together with the measurements of Ref [3]. We use here the parameters $A = -1.2 \pm 0.2$ [19, 20], and $B = 0.70 \pm 0.035$ [19-21], which lead to $J = 2.2 \pm 0.6$. The largest uncertainty is in A , owing to a systematic difference between the measurements [19, 20] of the pressure dependence of the density of dilute solutions.

We return now to justify neglecting viscous stresses in the pressure equation (4). The drag force per unit volume of the ^3He on the phonons is $\sim \rho_{ph}s/\ell_{ph3}$. We assume laminar flow in a circular pipe of radius R , for which $\nabla^2 \vec{v}_{ph} = -8\langle \vec{v}_{ph} \rangle / R^2$ is a constant throughout [22], thus overestimating the viscous force (density) on the phonons by neglecting the drag against the ^3He . The phonon viscosity is $\sim \rho_{ph}s\ell_{visc}/5$, where ℓ_{visc} is the phonon mean

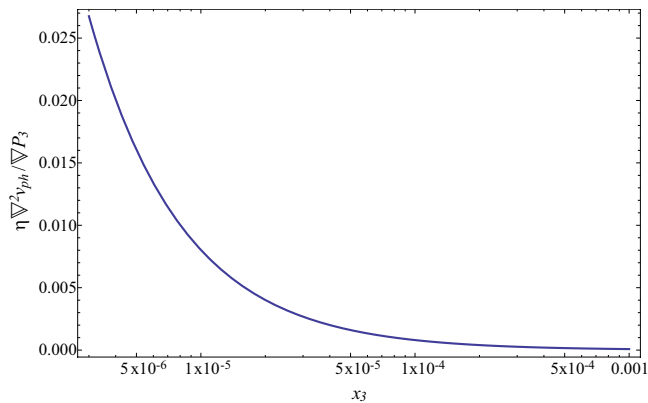


FIG. 2: Ratio of the contribution of the viscous term (see Eq. (4)) to the drag on the phonons due to scattering against the ^3He at a temperature of 0.45 K. The magnitude of the drag is given by the ^3He pressure gradient (see Eq. (25)) as a function of ^3He concentration x_3 (the concentrations measured in [4] are $x_3 = 7 \times 10^{-5}$ and 3×10^{-4}). The viscous term is calculated for laminar flow in a circular pipe of radius $R = 2.5$ cm, using the ^4He viscosity measured by Greywall [23].

free path for viscosity, and thus the ratio of the viscous force to drag force is $\sim \ell_{visc} \ell_{ph3} / R^2 \ll 1$; see Fig. 2. In addition, the ratio of the ^3He viscosity, $\sim m^* n_3 \bar{v} \ell_{33} / 5$ (where \bar{v} is a mean ^3He thermal velocity), to the phonon viscosity is of order $(n_3 / S_{ph})(\ell_{33} / \ell_{visc}) \ll 1$ here.

V. DIFFUSION OF ^3He AGAINST PHONONS

We now calculate the rate of diffusion of ^3He atoms in a bath of phonons at a fixed temperature T . In the derivation of heat transport above, we assumed that the ^3He cloud was at rest and that the phonons were drifting with velocity \vec{v}_{ph} . In a frame in which the phonons are at rest and the ^3He drift with velocity \vec{v}_3 , Eq. (25) becomes

$$\nabla P_3 = -\frac{n_3 \Gamma}{3T} \vec{v}_3, \quad (28)$$

where we use $\nabla P_{ph} = -\nabla P_3$. With the temperature variation in P_3 neglected, Eq. (28) becomes a familiar diffusion equation,

$$D_3 \nabla n_3 = -n_3 \vec{v}_3, \quad (29)$$

where

$$D_3 = \frac{3T^2}{\Gamma} \sim \frac{1}{T^7}. \quad (30)$$

More generally, however, phonons drive ^3He pressure gradients, rather than simply density gradients. In an arbitrary frame, the response of the ^3He current to a phonon wind becomes

$$\vec{j}_3 = n_3 \vec{v}_3 = n_3 \vec{v}_{ph} - D_3 \nabla n_3 - D_T \nabla T, \quad (31)$$

where, in our particular case, $D_T = n_3 D_3 / T$ is an effective “thermoelectric” transport coefficient.

VI. APPLICATION TO EXPERIMENT

To further illustrate the physics, we now determine the temperature and concentration distributions for two geometries (Refs. [3] and [4]) of interest. Conservation of energy implies

$$\nabla \cdot \vec{Q} = -\nabla \cdot (K_{ph} \nabla T) = -C \nabla \left(\frac{\nabla T}{P_3} \right) = 0, \quad (32)$$

where, from Eq. (27), $C = n_4^2 s^2 / 90 \pi J$. For simplicity, recoil effects are neglected in writing the equations here; however, they are taken into account in all numerical calculations reported below. We eliminate P_3 using the solution

$$P_3 + \frac{1}{4} S_{ph} T = P, \quad (33)$$

of Eq. (6), where the constant P is the total pressure of the excitations. Equation (32) then reduces to a partial differential equation in T alone (even when including the recoil corrections), which we solve using the finite element code FlexPDE [24]. Given $T(\vec{r})$, we determine $n_3(\vec{r})$ from Eq. (33), and determine the constant P by fixing the total number of ^3He atoms in the system.

We begin by applying this theoretical description to the experiment of Rosenbaum et al. [3], where the thermal conductivity of mixtures in the concentration range $1.1 \times 10^{-4} \leq x_3 \leq 1.3 \times 10^{-2}$ were measured at temperatures $0.084 \leq T \leq 0.65$ K. They determined the thermal conductivity by measuring the temperature difference over a 5 cm length of pipe, 0.26 cm in diameter, in the presence of a localized heat source. The pipe was connected to small reservoirs at either end containing the thermometers, the coupling to the dilution refrigerator and the heater.

In the analysis in Ref. [3], the effect of the variable ^3He concentration in the pipe, and its attendant effect on the thermal conductivity, was not taken into account. We therefore determined the temperature and concentration distributions in their system by adjusting the heater power and minimum (dilution refrigerator) temperature to match the reported average temperature and the temperature difference implied by the reported thermal conductivity. We note that the ^3He thermal conductivity is negligibly small owing to $\ell_{33} \ll \ell_{3ph}$, Eq. (19).

Because the phonons push the ^3He into the cold reservoir, the average concentration in the pipe is substantially lower than the concentration including the reservoirs. We show the results of our calculations in Fig. 1 for representative measurements [25] of Ref. [3]. The open circles are the thermal conductivities as reported, plotted at the average overall concentration; the solid circles are plotted at the average concentrations calculated for the pipe. Because the dimensions of the reservoirs are not given in Ref. [3], there is some uncertainty in the calculated result. The error bars shown in Fig. 1 represent changes of about $\pm 25\%$ from the reservoir volumes estimated from the schematic in their Fig. 1. Given

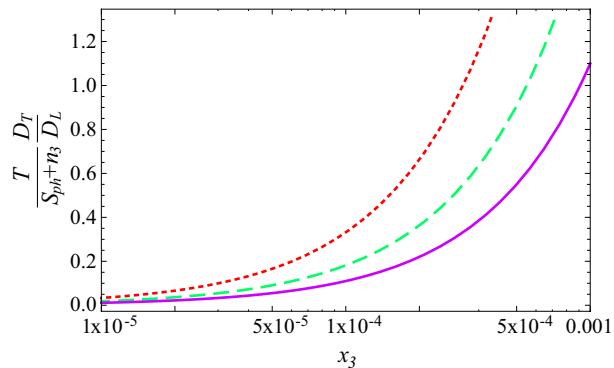


FIG. 3: (Color online) Contribution of the thermoelectric transport term relative to the effective diffusion constant, D_L extracted in Ref. lamoreaux. The temperatures are 0.45 K (dotted), 0.55 K (dashed) and 0.65 K (solid).

the uncertainties related to the geometry and the details of how the thermal conductivity was extracted, there is good agreement between this calculation and the measurement. As previously noted in Sec. III, the theoretical analysis in Ref. [3] incorrectly assumed that the primary phonon relaxation was due to ^3He -phonon scattering, rather than phonon-phonon scattering along rays.

We now analyze the experiment of Lamoreaux et al. [4], which measures the ^3He density response to a localized heat source by a novel technique. In the experiment, a dilute solution with concentration in the range 7×10^{-5} to 3×10^{-4} is contained in a cylindrical cell roughly 5 cm in diameter and 5 cm long, cooled at one end by a dilution refrigerator to a temperature T in the range 0.45 – 0.95 K [26]. A temperature gradient is created by a resistive heater generating 7–15 mW, located roughly midway between the ends and near the cylinder wall (see Fig. 4 below). The resulting spatial distribution of the ^3He density is probed by a well-collimated neutron beam of diameter ~ 0.25 cm going through the cell. A fraction of the neutrons are captured via the reaction $n + ^3\text{He} \rightarrow p + t + 764$ keV. The XUV scintillation light from protons and tritons in the liquid ^4He is converted to visible light and detected by a photomultiplier tube which views the solution through a window at the other end of the cell. The yield of scintillation light, measured as a function of cell temperature, initial ^3He concentration, and heater power, is used to determine the thermally induced change in the ^3He distribution. The heat flow again produces non-uniform temperature and ^3He concentration distributions. Because the concentration and temperature gradients are directly proportional, Eq. (7), the concentration gradients implied by the measured scintillation yields here simply encode the same type of temperature difference information measured by Rosenbaum et al. We note that the proportionality constant involves $S_{ph} + n_3$, rather than just S_{ph} .

The response of the ^3He density to the heat source is given here by Eq. (8). Combining this result with $\vec{Q} =$

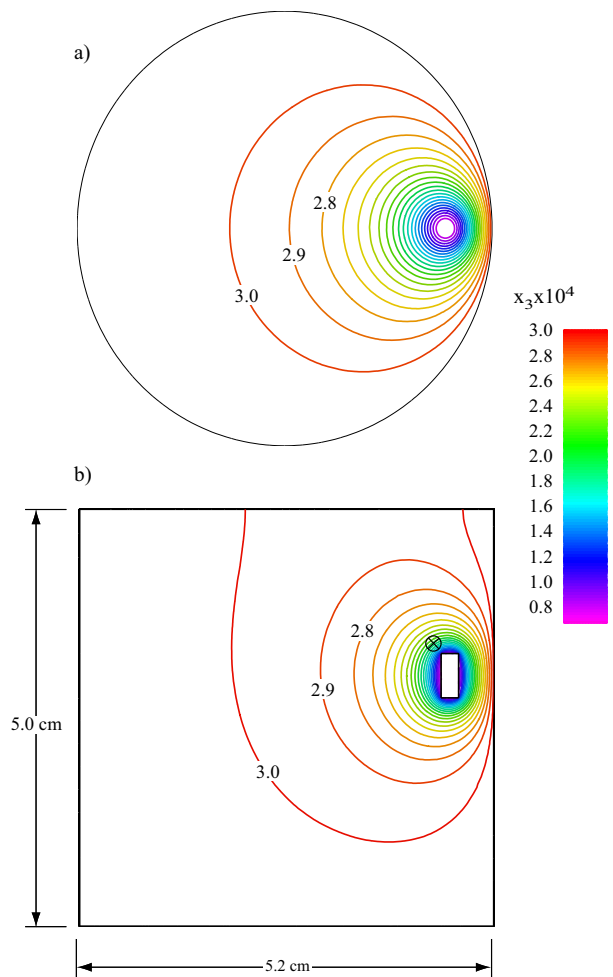


FIG. 4: (Color online) An example of the ^3He distribution for a cell 5.2 cm in diameter and 5.0 cm high, with refrigerator temperature 0.45 K, average $x_3 = 3 \times 10^{-4}$, and heater power 15 mW. The sections are: a) perpendicular to the cylinder axis and containing the neutron beam axis; and b) perpendicular to the neutron beam (the cross in the figure) and through the center of the heat source. We assume in this simulation that the cylindrical wall of the cell is at the same temperature as that of the base where the refrigerator is attached; the top surface is insulated. The ^3He concentration contours, of constant spacing, are marked in units of 10^{-4} ; the minimum is $x_3 = 0.69 \times 10^{-4}$ at the surface of the heater and the maximum concentration is 3.05×10^{-4} , on the lower cell boundary.

$TS_{ph}\vec{v}_{ph}$, one can write

$$\nabla n_3 = \frac{S_{ph}(S_{ph} + n_3)}{K} \vec{v}_{ph}. \quad (34)$$

Reference [4], which did not take into account the temperature gradient induced by the heat flow, interpreted the result for the ^3He density gradient in terms of a simple diffusion constant, D_L , in the form,

$$\nabla n_3 = \frac{n_3}{D_L} \vec{v}_{ph}. \quad (35)$$

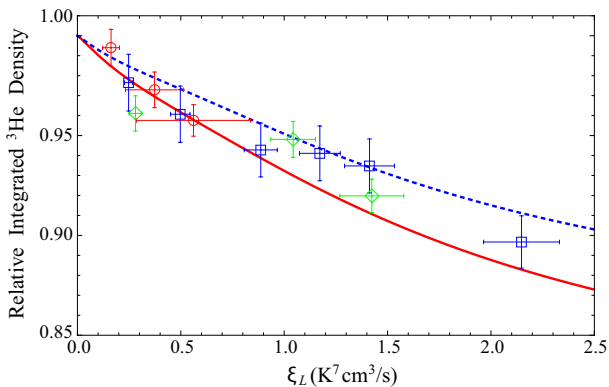


FIG. 5: (Color online) Representative results of the finite element calculation, including ${}^3\text{He}$ recoil, of the relative integrated ${}^3\text{He}$ (column) density along the neutron beam as a function of the quantity $\xi_L = T^7 (\mathcal{P}/S_{ph}T)$ where \mathcal{P} is the heater power, along with data from Ref. [4] (circles, 0.45 K; diamonds, 0.55 K and squares, 0.65 K). The curves are for a refrigerator (and barrel) temperature of 0.45 K: *solid*, $x_3 = 3 \times 10^{-4}$; *dotted*, $x_3 = 7 \times 10^{-5}$; coincidentally, the results for $T = 0.65$ K and $x_3 = 3 \times 10^{-4}$ are essentially the same as the dotted curve. The curves are plotted for the average temperature (greater than the boundary temperature) along the neutron beam path. For example, at the actual value $T^6\mathcal{P}/S_{ph} = 2.5$, the average ξ_L is shifted upward by $\Delta\xi_L \approx 0.05 \text{ K}^7 \text{ cm}^3/\text{s}$ for $T = 0.45$ K, and by $\Delta\xi_L \approx 0.5 \text{ K}^7 \text{ cm}^3/\text{s}$ for $T = 0.65$ K.

From Eq. (34) we see that

$$D_L = \frac{n_3}{S_{ph} + n_3} \frac{K}{S_{ph}}. \quad (36)$$

Equivalently,

$$D_L = D_3 - \frac{T}{S_{ph} + n_3} D_T = \frac{S_{ph}}{S_{ph} + n_3} D_3. \quad (37)$$

The D_T term in this equation makes a significant contribution at higher concentrations (see Fig. 3); as noted, $n_3 \sim S_{ph}$ for a large range of concentrations in the experiment of Ref. [4]. This effective D_L is not a simple diffusion constant, owing to the presence of the temperature gradient. We note that while the temperature dependence of the result for D_3 without ${}^3\text{He}$ recoil falls with temperature as $1/T^7$, the temperature dependence of the effective D_L differs, owing both to recoil effects and the $1/T^3$ dependence of n_3/S_{ph} . The relative similarity of D_L and D_3 also depends on the ${}^3\text{He}$ thermal conductivity being negligible.

An example of the ${}^3\text{He}$ distribution resulting from the finite element calculation for the Lamoreaux et al. experiment is shown in Fig. 4; results of the relative integrated (column) ${}^3\text{He}$ densities along the neutron beam are shown in Fig. 5 together with the data in Fig. 4 of [4]. To illustrate the effect of other variables in the problem, we also show in Fig. 5 the results for $T = 0.65$ K and for the two concentrations used in the experiment. In this

calculation we take the refrigerator end and the barrel of the cell to be fixed at $T = 0.45$ and 0.65 K as indicated; the opposite end of the cell is insulated. We note that the conductivity of the aluminum barrel is more than an order of magnitude larger than that of the phonons at these temperatures [27]. The relative column density calculated with an insulator in place of the aluminum barrel (not shown) falls well below the data. In this simulation we neglect any possibility of convective flow in the ${}^3\text{He}$. The effect of the non-zero size of the neutron beam is to reduce the calculated ratios in Fig. 5 by ~ 0.003 at the largest values of ξ_L , well within the reported uncertainties. The agreement of the present theory with the experiment provides further confirmation of the microscopic transport theory in the concentration range of the Lamoreaux et al. experiment.

VII. SUMMARY

We have laid out the basic transport theory of dilute solutions of ${}^3\text{He}$ in superfluid ${}^4\text{He}$ in the regime where scattering among the ${}^3\text{He}$ is the primary mechanism keeping the ${}^3\text{He}$ in thermal equilibrium, and phonons are the significant excitations of the ${}^4\text{He}$. We find that in the range of ${}^3\text{He}$ concentrations in the Rosenbaum et al. [3] and Lamoreaux et al. [4] experiments, $7 \times 10^{-5} \leq x_3 \leq 1.5 \times 10^{-3}$, heat transport is dominated by phonons. The physical response of the system is not simple diffusion, described only by a ${}^3\text{He}$ diffusion constant, D_3 , since the temperature gradients are important. The experiments can be characterized simply by a phonon thermal conductivity. This thermal conductivity, calculated in a microscopic framework, satisfactorily reproduces the measurements, indicating that the well-tested theory of ${}^3\text{He}$ -phonon scattering in dilute solutions of ${}^3\text{He}$ in superfluid ${}^4\text{He}$ is consistent with these experiments as well.

Acknowledgments

This research was supported in part by NSF Grants PHY-0701611, PHY-0855569, PHY-0969790 and PHY-1205671. We thank the authors of [4], especially Robert Golub, Michael Hayden and Jen-Chieh Peng, for helpful discussions about the experiment. GB is grateful to the Aspen Center for Physics, supported in part by NSF Grant PHY-1066292, and the Niels Bohr International Academy where parts of this research were carried out. DB thanks Caltech, under the Moore Scholars program, where parts of this research were carried out.

Appendix A: Recoil corrections

In this Appendix we calculate contributions to the thermal conductivity due to the finite ${}^3\text{He}$ mass. We

start from Eq. (24) with the structure factor (22) of the ${}^3\text{He}$,

$$\begin{aligned}\nabla P_{ph} &= -\vec{v}_{ph} \frac{2\pi n_3}{6T} \int \frac{d^3q}{(2\pi)^3} \int \frac{d^3q'}{(2\pi)^3} n_q^0 (1 + n_{q'}^0) k^2 |\langle T \rangle|^2 \left(\frac{m^*}{2\pi k^2 T} \right)^{1/2} e^{-m^*(sq - sq' - k^2/2m^*)^2/2k^2 T}. \\ &= -\vec{v}_{ph} \frac{2\pi n_3}{6T} \int \frac{d^3q}{(2\pi)^3} \int \frac{d^3q'}{(2\pi)^3} \frac{k^2 |\langle T \rangle|^2}{4 \sinh(sq/2T) \sinh(sq'/2T)} \left[\left(\frac{m^*}{2\pi k^2 T} \right)^{1/2} e^{-m^*(sq - sq')^2/2k^2 T} \right] e^{-k^2/8m^* T}.\end{aligned}\tag{A1}$$

The integral in Eq. (A1) is proportional to the inverse of the thermal conductivity. In the limit $m^* \rightarrow \infty$ the expression in square brackets reduces to $\delta(sq - sq')$. For finite m^* there are two effects. First, the structure factor, and therefore also the scattering rate, is reduced in magnitude because of the nonzero momentum transfer, $\vec{k} = \vec{q} - \vec{q}'$, as is shown by the final Gaussian factor. Second, as the first Gaussian factor indicates,

there is an energy transfer $sq - sq'$ which is of order $(Tk^2/m^*)^{1/2} \sim (T/m^*s^2)^{1/2}T$.

The contributions to the scattering amplitude for nonzero energy transfer and for nonzero velocity of the ${}^3\text{He}$ atoms have not been investigated in detail, although the basic processes were discussed in full in Ref. [7]. Here we use Eq. (13) for the scattering amplitude. With prefactors omitted, the quantity to be calculated is thus

$$\int_0^\infty dq \int_0^\infty dq' \int_{-1}^1 d\cos\theta \frac{k(qq')^3 (A + B \cos\theta)^2}{4 \sinh(sq/2T) \sinh(sq'/2T)} e^{-m^*s^2(q-q')^2/2k^2T} e^{-k^2/8m^*T}.\tag{A2}$$

We have evaluated the integrals numerically and find, as stated in Sec. IV, that inclusion of recoil effects increases the thermal conductivity by $\sim 25 - 35\%$ in the temperature range $0.45 - 0.65$ K.

The leading corrections to the result for $m^* \rightarrow \infty$ are of relative order T/m^*s^2 relative to the result in the low temperature limit; we now calculate them analytically. To first order in T/m^*s^2 the effects of the nonzero momentum transfer and the nonzero energy transfer are additive, and we calculate each in turn. The more important term is due to the momentum transfer. When this term alone is included one finds

$$\lim_{T \rightarrow 0} (TK)/TK \simeq 1 - \frac{1}{8m^*T} \frac{\langle k^4 \rangle}{\langle k^2 \rangle},\tag{A3}$$

where

$$\langle \dots \rangle = \int_0^\infty dq \int_{-1}^1 d\cos\theta \frac{q^6 (A + B \cos\theta)^2}{4 \sinh^2(sq/2T)} (\dots).\tag{A4}$$

In these integrals we may replace k^2 by its value $2q^2(1 - \cos\theta)$ for zero energy transfer. The integrals over q and θ decouple and one finds

$$TK \simeq \left(1 + \frac{T}{4m^*s^2} \frac{\tilde{J} I_{10}}{J I_8} \right) \lim_{T \rightarrow 0} (TK),\tag{A5}$$

where

$$\begin{aligned}\tilde{J} &= \int_{-1}^1 \frac{d\cos\theta}{2} (A + B \cos\theta)^2 (1 - \cos\theta)^2 \\ &= \frac{4}{3}A^2 - \frac{4}{3}AB + \frac{8}{15}B^2\end{aligned}\tag{A6}$$

and

$$I_n = \int_0^\infty dq \frac{x^n}{4 \sinh^2(x/2)} = n! \zeta(n),\tag{A7}$$

where $\zeta(n)$ is the Riemann zeta function of order n . Therefore the thermal conductivity is given by

$$K \simeq \left(1 + \frac{25\pi^2 \tilde{J}}{11} \frac{T}{J m^*s^2} \right) \frac{1}{T} \lim_{T \rightarrow 0} (TK).\tag{A8}$$

We now calculate the leading correction to the thermal conductivity due to the energy transfer, which is found by neglecting the term $k^2/8m^*T$ in the exponent in Eq. (A2). The Gaussian in the energy difference has a width small compared with T , so we adopt a procedure similar to that used in making the Sommerfeld expansion for low temperature Fermi systems, where the derivative of the Fermi function approaches a delta function. In an integral of the form,

$$G(x) = \int_0^\infty dy g(y) \frac{e^{-(x-y)^2/2\Delta^2}}{(2\pi\Delta)^{1/2}},\tag{A9}$$

where Δ is a constant, and the function $g(y)$ varies slowly on the scale Δ , one finds on expanding g in a Taylor series about $y = x$, that

$$G(x) = g(x) + \frac{\Delta^2}{2}g''(x) + \dots \quad (\text{A10})$$

When this result is applied to the q' integral in Eq. (A2) with the final Gaussian omitted, one finds

$$\begin{aligned} & \int_0^\infty dq \int_0^\infty dq' \int_{-1}^1 \frac{d \cos \theta}{2} \left(\frac{m^* s^2}{2\pi T k^2} \right)^{1/2} \frac{k^2 (qq')^3 (A + B \cos \theta)^2 e^{-m^* s^2 (q-q')^2 / 2k^2 T}}{4 \sinh^2(sq/2T)} \\ \simeq & J \int_0^\infty dq \frac{2q^8}{4 \sinh^2(sq/2T)} + \frac{T}{2m^* s^2} \int_0^\infty dq \int_{-1}^1 \frac{d \cos \theta}{2} \frac{k^2 q^3 k^2 (A + B \cos \theta)^2}{2 \sinh(sq/2T)} \left(\frac{\partial^2}{\partial (q')^2} \frac{k^2 q^3}{2 \sinh(sq'/2T)} \right)_{q'=q}, \quad (\text{A11}) \end{aligned}$$

which, when expressed in terms of the variables $x = sq/T$, $y = sq'/T$, and $z = \cos \theta$, is proportional to

$$J \int_0^\infty dx \frac{2x^8}{4 \sinh^2(x/2)} + \frac{T}{m^* s^2} \int_0^\infty dx \frac{x^5}{2 \sinh(x/2)} \int_{-1}^1 \frac{dz}{2} (1-z)(A+Bz)^2 \left(\frac{\partial^2}{\partial y^2} \frac{\kappa^2 y^3}{2 \sinh(y/2)} \right)_{y=x}, \quad (\text{A12})$$

where $\kappa^2 = x^2 + y^2 - 2xyz$. The second derivative is

$$\frac{x^3}{\sinh(x/2)} \left\{ 1 + (1-z) \left[12 - \frac{1}{4}x^2 - 4x \coth(x/2) + \frac{1}{2}x^2 \coth(x/2)^2 \right] \right\}. \quad (\text{A13})$$

On evaluating the integrals, one finds that the effect of energy transfer produces contributions to the integral (A2) having the form

$$1 + \left(1 - \frac{(25\pi^2 - 198)\tilde{J}}{33} \right) \frac{T}{m^* s^2}. \quad (\text{A14})$$

The numerical factor $(25\pi^2 - 198)/33$ is approximately 1.477 and thus one sees that the effects of nonzero energy transfer are much less important than those due to nonzero momentum transfer. When both contributions to the thermal conductivity are included, one finds on inserting Eq. (27) for the low temperature limiting behavior,

$$K \simeq \frac{n_4 s^2}{90\pi x_3 J T} \left(1 + \frac{T}{m^* s^2} \left[\frac{100\pi^2 - 198\tilde{J}}{33} \frac{\tilde{J}}{J} - 1 \right] \right). \quad (\text{A15})$$

The coefficient of \tilde{J}/J is approximately 23.90. For $A = -1.2$ and $B = 0.70$, J is 2.16, \tilde{J} is 3.30 and their ratio is 1.52. Thus the coefficient of $T/m^* s^2$ is 35.5. Even though $m^* s^2 = 48.1$ K, the effects of recoil are large even at temperatures well below 1 K as a consequence of the large numerical coefficient. This coefficient reflects the fact that the most important contributions to the momentum transfer arise from phonons with momenta $\gg T/s$. At $T = 0.5$ K the correction is 37%, which is considerable. Higher-order contributions in T can be significant, and one would expect these to reduce the deviation from the low-temperature limiting result by an amount of relative order $(0.37)^2 \sim 10\%$. These analytic results are in good agreement with the numerical integration of Eq. (A2) described above, and shown in Fig. 1.

-
- [1] R. Golub and S. K. Lamoreaux, Phys. Rep. **237**, 1 (1994).
[2] This experiment utilizes the absorption of ultracold polarized neutrons on polarized ^3He atoms via the reaction $n + ^3\text{He} \rightarrow p + t + 764$ keV.
[3] R. L. Rosenbaum, J. Landau and Y. Eckstein, J. Low Temp. Phys. **16**, 131 (1974).
[4] S. K. Lamoreaux, G. Archibald, P. D. Barnes, W. T. Buttler, D. J. Clark, M. D. Cooper, M. Espy, G. L. Greene, R. Golub, M. E. Hayden, C. Lei, L. J. Marek, J.-C. Peng, and S. Penttila, Europhys. Lett. **58**, 718 (2002).
[5] M. Hayden, S. K. Lamoreaux, and R. Golub, AIP Conf. Proc. **850**, 147 (2006).
[6] G. Baym, D. H. Beck, and C. J. Pethick, to be published.
[7] G. Baym and C. Ebner, Phys. Rev. **164**, 235 (1967).
[8] H. J. Maris, Rev. Mod. Phys. **49**, 341 (1977).
[9] G. Baym, R. G. Barrera, and C. J. Pethick, Phys. Rev. Lett. **22**, 20 (1969).
[10] R. M. Bowley, Europhys. Lett. **58**, 725 (2002).

- [11] The phonon contributions to the dissipative second viscosity terms in the superfluid acceleration equation vanish, see [12].
- [12] I. M. Khalatnikov, *Introduction to the Theory of Superfluidity*, (W. A. Benjamin, New York, 1965), pp. 65,133.
- [13] I. M. Khalatnikov, *op. cit.*, ch. 25; I. M. Khalatnikov and V. N. Zharkov, Zh.E.T.F. **32**, 1108 (1957) [Engl. transl. Sov. Phys. JETP **5**, 905 (1957)].
- [14] J. Wilks, *The Properties of Liquid and Solid Helium*, (Clarendon Press, Oxford, 1967), sec. 9.5.
- [15] L. D. Landau and E. M. Lifshitz, *Fluid Mechanics* (Pergamon Press, 1987), Sec. 59.
- [16] G. Baym and C. Ebner, Phys. Rev. **170**, 346 (1968).
- [17] Note that in the implementation of this correction in Ref. [10], the ^3He effective mass is taken to be one third of its actual value, and therefore the effects of recoil are overestimated.
- [18] One should not be alarmed by the apparent divergence as $x_3 \rightarrow 0$. When x_3 becomes sufficiently small, the ^3He no longer provide the mechanism for absorbing momentum from the phonons, and rather the phonon thermal conductivity becomes limited by viscous transfer of momentum from the phonons to the container walls [6].
- [19] C. Boghosian and H. Meyer, Phys. Lett. **A25**, 352 (1967).
- [20] G. E. Watson, J. D. Reppy, and R. C. Richardson, Phys. Rev. **188**, 384 (1969).
- [21] B. M. Abraham, C. G. Brandt, Y. Eckstein, J. Munarin, and G. Baym, Phys. Rev. **188**, 309 (1969).
- [22] In fact, the viscosity for flow in a circular pipe plays a role only in a thin boundary layer, which for the concentrations and temperatures under consideration is of order mm thick.
- [23] D. S. Greywall, Phys. Rev. B **23**, 2152 (1981).
- [24] PDE Solutions Inc., Spokane Valley, WA 99206 USA.
- [25] We note that the analysis here must be extended for the lower temperatures in the experiment to include scattering from the walls. For example, the phonon mean free path is larger than the diameter of the pipe for temperatures below about 0.37 K.
- [26] We are grateful to M. Hayden, private communication, for the details of the geometry.
- [27] C. B. Satterthwaite, Phys. Rev. **125**, 873 (1962), R. M. Mueller, C. Buchal, T. Oversluizen, and F. Pobell, Rev. Sci. Instrum. **49**, 515 (1978) and references therein.